Talanta 90 (2012) 91–98

Contents lists available at SciVerse ScienceDirect

Talanta

journal homepage: www.elsevier.com/locate/talanta

Electrocatalytic oxidation of NADH at electrogenerated NAD^+ oxidation product immobilized onto multiwalled carbon nanotubes/ionic liquid nanocomposite: Application to ethanol biosensing

Hazhir Teymourian[a,c], Abdollah Salimi[a,b,*], Rahman Hallaj[a]

[a] Department of Chemistry, University of Kurdistan, P.O. Box 416, Sanandaj, Iran
[b] Research Center for Nanotechnology, University of Kurdistan, P.O. Box 416, Sanandaj, Iran
[c] Department of Chemistry, University of Tarbiat Modarres, Tehran, Iran

ARTICLE INFO

Article history:
Received 21 October 2011
Received in revised form
18 December 2011
Accepted 1 January 2012
Available online 5 January 2012

Keywords:
Electrogenerated NAD^+ oxidation products
MWCNTs
Ionic liquid
NADH
Ethanol
Biosensor

ABSTRACT

The multiwalled carbon nanotubes/N-butyl-N-methyl-pyrolydinium-bis(trifluoromethylsulfonyl)imide [C_4mpyr][NTf_2] ionic liquid (MWCNTs/IL) modified glassy carbon (GC) electrode has been utilized as a platform to immobilize electrogenerated NAD^+ oxidation products (Ox-P(NAD^+)). During potential cycling, the adenine moiety of NAD^+ molecule is oxidized and gives rise to generation of a redox active system that shows great electrocatalytic activity toward NADH oxidation. The cyclic voltammetric results indicated the ability of MWCNTs/IL/Ox-P(NAD^+) modified GC electrode to catalyze the oxidation of NADH at a very low potential (0.05 V vs. Ag/AgCl) and subsequently, a substantial decrease in the overpotential by about 600 mV compared with the bare GC electrode. This modified electrode thus allowed highly sensitive amperometric detection of NADH with a very low limit of detection (2×10^{-8} mol L^{-1}), low applied potential (+0.05 V) at concentration range up to 4.2×10^{-5} mol L^{-1} and minimum of surface fouling. High ability of MWCNTs/IL/Ox-P(NAD^+) to promote electron transfer between NADH and the electrode suggested a new promising biocompatible platform for development of dehydrogenase-based amperometric biosensors. With alcohol dehydrogenase (ADH) as a model enzyme, ethanol sensing ability of the proposed system was examined. The amperometric response of the biosensor increased linearly with increasing ethanol concentration in two concentration ranges, 5×10^{-6}–6×10^{-5} and 6×10^{-5}–9×10^{-4} mol L^{-1} with detection limit of 5×10^{-7} mol L^{-1} and rapid response of 10 s. Furthermore, the interference effects of redox active species, such as ascorbic acid, uric acid, glucose and acetaminophen for the proposed biosensor are negligible. Finally, the ability of the proposed biosensor for detection of ethanol in real complex samples was successfully demonstrated.

1. Introduction

Because over 300 dehydrogenases require nicotinamide coenzymes as cofactors, the electrocatalytic oxidation of β-nicotinamide adenine dinucleotide (NADH) has been of particular interest [1]. NADH and its oxidized form, NAD^+, are the key central charge carriers in living cells. In addition, the development of such electrocatalysts could be coupled to biosensor design for the determination of numerous species [2–5]. Although the reversible potential of the NADH/NAD^+ redox couple is estimated to be −0.32 V (vs. NHE) [6], direct electrochemical oxidation of NADH at bare electrodes, such as gold, platinum and carbon always features a high overpotential owing to the sluggish charge transfer kinetics, which greatly limits the practical application of the corresponding biosensors due to the deterioration of selectivity [7,8]. Such a high overpotential also yields some physiologically inactive dimmers which contaminate the electrode surfaces and finally causes electrode fouling [9]. Thus, use of electron-transfer mediators along with the development of new electrode materials with improved electrochemical properties is some of the most frequently used strategies to overcome the aforementioned difficulties [10]. In this way, much effort has been dedicated in the last few decades to identify materials which can effectively overcome the kinetic barriers for electrochemical regeneration of NAD^+. Water soluble dye compounds [11–13], catechol and quinone derivatives [14–16], phenothiazine derivatives [17,18], phenyl azo aniline [19], adenine derivatives [2,20] and various redox polymers [21–25] are some of the different electron transfer mediators that have been used for electrocatalytic oxidation of NADH.

With respect to the construction of an electrochemical biosensor, it is more attractive to immobilize the electron transfer

* Corresponding author at: Department of Chemistry, University of Kurdistan, P.O. Box 416, Sanandaj, Iran. Tel.: +98 871 6624001; fax: +98 871 6624008.
E-mail addresses: absalimi@uok.ac.ir, absalimi@yahoo.com (A. Salimi).

0039-9140/$ – see front matter © 2012 Elsevier B.V. All rights reserved.
doi:10.1016/j.talanta.2012.01.003

mediator on the transducer to give rise to a more compact and simple sensory configuration. Modifying the electrode surface with nanomaterials (including nonparticles, nanotubes, nanorods, etc.) allows efficient electron transfer between the matrix electrode and redox proteins or enzymes [26]. Among different nanomaterials, carbon nanotubes (CNTs) are considered as an important group of nanostructures with attractive electronic, chemical and mechanical properties [27,28]. These unique properties make them extremely attractive for fabricating chemical sensors, in general, and electrochemical ones, in particular [29]. Furthermore, CNTs have been shown to impart good responses and minimization of surface fouling in electrochemical devices [30,31]. The compatibility and electrochemical applications of CNTs to immobilize a variety of species on their external and internal surfaces have been reported [32–36]. However, it is noted that CNTs, which have a high specific surface area, tend to form irreversible agglomerates through strong π–π stacking and van der Waals interaction [37]. Hence the prevention of aggregation is a key challenge in the synthesis and processing of bulk quantity of CNTs. Ionic liquids (ILs) can meet this challenge well. Due to the high stability and electrical conductivity, very low vapor pressure and wide electrochemical window, ILs holds a great promise for various electrochemical applications [38–41]. ILs can be applied either as an electrolyte, a modifier on the electrode surface or as a binder to prepare the carbon paste electrode for broad electrochemical applications. CNTs can be well dispersed in ILs due to cation–π interactions and a CNTs–ILs paste can easily be prepared using ILs as the binder, where the CNTs greatly enhances the conductivity of the system [42,43]. Through combining the benefits of ILs and CNTs for electrochemical sensing applications, a remarkable synergistic augmentation of electrochemical performance can be achieved.

In our earlier work, we made it possible to successfully catalyzing NADH electrooxidation using electrogenerated chloropromazine oxidation product as an efficient electron mediator on the surface of MWCNTs/IL nanocomposite modified glassy carbon electrode [44]. The capability of the System for ethanol detection was also reported when enzyme alcohol dehydrogenase integrated into the nanocomposite. However, low sensitivity, instability and rather high oxidation potential of NADH were main disadvantages of the chloropromazine based ethanol biosensor. Moreover, it has been shown by Alvarez-Gonzales and coworkers that through electrochemical oxidation of the adenine moiety in NAD^+ molecules at potentials as high as 1.2 V in alkaline solutions, an oxidation product was obtained which showed high electrocatalytic activity for NADH oxidation [2]. In the present paper, we extended our previous work by introducing the oxidation product of NAD^+ as a surface immobilized redox system through integration of room-temperature ionic liquid and MWCNTs to generate a nanocomposite-based biosensor with excellent electrocatalytic activity for NADH electrooxidation. Our proposed biosensor was fabricated using N-butyl-N-methyl pyrolydinium bis (trifluoromethylsulfonyl) imide [C_4mpyr][NTf_2] (IL) as the binder, MWCNTs as the conduit and oxidation product of NAD^+ as the redox mediator. This new nanocomposite has several advantages compared to other conventional electrodes. The interaction between MWCNTs and IL results in the formation of a robust composite electrode with a low background current. Electrochemical oxidation of NAD^+ on MWCNTs/IL nanocomposite as transducer led to a significant improvement in terms of sensitivity, stability, detection limit and linear range for electrocatalytic oxidation of NADH. Using alcohol dehydrogenase (ADH) as a model enzyme, the possibility of coupling MWCNTs/IL/Ox-P(NAD^+) electrocatalytic system for NADH to the reaction catalyzed by dehydrogenase enzymes for the preparation of an ethanol biosensor was examined. The detection of ethanol in the presence of redox active interferences such as ascorbic acid, uric acid, glucose and acetaminophen was also realized.

2. Experimental

2.1. Chemicals and reagents

N-butyl-N-methyl pyrolydinium bis (trifluoromethylsulfonyl) imide [C_4mpyr][NTf_2] (IL), NAD^+, NADH and alcohol dehydrogenase from baker's yeast (ADH, EC 1.1.1.1, 300 U mg^{-1}) was purchased from Sigma. Multiwalled carbon nanotubes (MWCNTs) with purity of 95%, surface specific area of 480 m^2 g^{-1}, diameter of 20–30 nm and 1 μm length were obtained from Nanolab (Brighton, MA). Phosphate buffer solutions (PBS, 0.1 mol L^{-1}) with different pHs were prepared with NaH_2PO_4 and Na_2HPO_4 and used as supporting electrolyte throughout electrochemical studies. pH adjustment was performed with NaOH or HCl. Uric acid (UA), ascorbic acid (AA), glucose (GL) and acetaminophen (AP) were prepared from Sigma. All aqueous solutions were prepared with ultra-pure water (≥18 MΩ cm) from a Milli-Q Plus system (Millipore). All other solvents were used as supplied (analytical or HPLC grade) without further purification.

2.2. Apparatus

Surface morphology was examined using Vega-Tesacn electron microscope (SEM). Cyclic voltammograms were performed using an AUTOLAB modular electrochemical system (ECO Chemie, Ultrecht, The Netherlands) equipped with a PGSTAT 101 module and driven by NOVA software (ECO Chemie) in conjunction with a conventional three-electrode system and a personal computer for data storage and processing. A modified glassy carbon electrode employed as the working electrode and a platinum wire as the counter electrode. All potentials were referred to an Ag/AgCl/KCl (3 M) electrode. Amperograms were carried out with a Metrohm multi-purpose instrument model 693VA processor, equipped with a 694VA stand. A Metrohm drive shaft was used to rotate working electrodes during amperometric detection. All electrochemical measurements were performed at ambient temperature of 20.0 ± 0.1 °C.

2.3. Preparation of MWCNTs/IL/Ox-P(NAD^+) modified GC electrode

Prior to coating, GC electrode was carefully polished before each experiment with 3.0 μm alumina powder on polishing cloth and sonicated successively in ethanol and doubly distilled water in order to remove adsorbed particles, then allowed to dry at room temperature. The nanocomposite was prepared by direct mixing of 20 μL IL and 0.5 mg of MWCNT on a glass slide so that a homogeneous paste obtained. The MWCNTs/IL modified GC electrode was fabricated by rubbing some of this paste on the electrode surface to form a homogeneous layer. The effective surface area of the electrode modified with MWCNTs/IL was determined as 0.13 cm^2 from cyclic voltammogram of 1 mM K_3 [$Fe(CN)_6$] in 0.1 mol L^{-1} PBS (pH 7). In order to oxidizing NAD^+ and immobilizing its oxidation product on the electrode surface, the potential of MWCNTs/IL modified GC electrode was cycled (5 cycles) between −0.4 and +1.5 V vs. Ag/AgCl at 0.1 V s^{-1} in a 0.1 mol L^{-1} PBS (pH 8.8) containing 1×10^{-3} mol L^{-1} NAD^+.

2.4. Ethanol biosensing procedure and real sample analysis

Scheme 1 shows the protocol used for ethanol biosensing with the MWCNTs/IL/Ox-P(NAD^+) modified GC electrode in a solution containing ADH and NAD^+. The enzymatic reactions involved in the biosensing system are as follows:

$$\text{Ethanol} + NAD^+ \xrightarrow{\text{ADH}} \text{Acetaldehide} + \text{NADH} + H^+ \quad \text{(R1)}$$

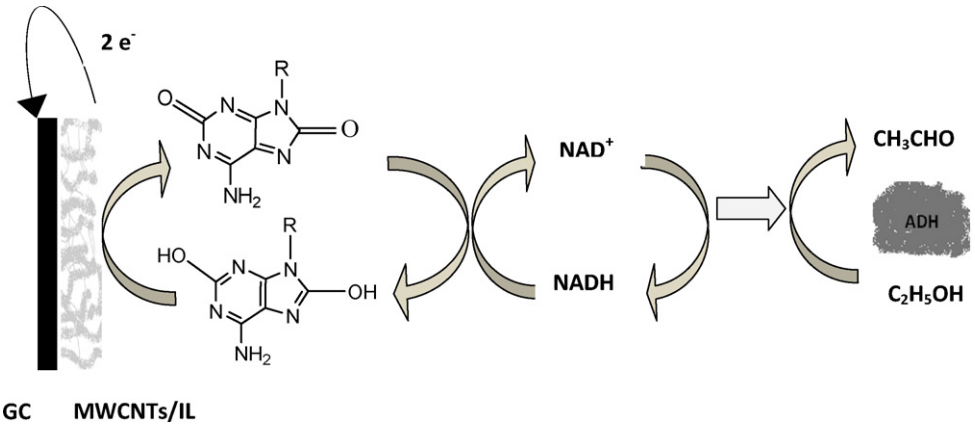

Scheme 1. Schematic representation for the bioelectrocatalytic sensing of ethanol using MWCNTs/IL/Ox-P(NAD^+) modified GC electrode.

$$NADH + MWCNTs/IL/Ox\text{-}P(NAD^+) \rightarrow NAD^+ + MWCNTs/IL/Ox\text{-}P(NAD^+) \quad (R2)$$

Here, enzyme alcohol dehydrogenase (ADH) catalyzes the oxidation of ethanol while the cofactor NAD^+ get reduced to NADH. The NADH generated in the enzymatic reaction is oxidized at the modified electrode. Since the concentrations of NAD^+ and its oxidation products at the surface of electrode are constant, the increase in the electrocatalytic current only depends on the ethanol concentration. Moreover, the proposed ethanol biosensor was applied to the measurement of ethanol concentration in three samples (lemon- and apple-flavored) of widely drunk beverages commercially named Istak and Delster. The samples were provided from the market and diluted 10 times with 0.1 mol L^{-1} PBS (pH 8.8) prior to measurements. The standard addition method was adopted to demonstrate the possibility of ethanol detection in real samples.

3. Results and discussion

3.1. Characterization and electrochemical properties of MWCNT/IL/Ox-P(NAD^+) modified GC electrode

The surface morphology of MWCNTs/IL modified GC electrode was investigated and the results were presented (supplier information S.1). As illustrated, the diameter of MWCNTs is in the range of 20–30 nm. However, when [C_4mpyr][NTf_2] as IL was added, the MWCNTs/IL nanocomposite exhibits a unique structure and forms a relatively uniform film.

For immobilization of NAD^+ oxidation products, the potential of MWCNTs/IL nanocomposite modified GC electrode was cycled in a 0.1 mol L^{-1} PBS (pH 8.8) containing 1×10^{-3} mol L^{-1} NAD^+ (Fig. 1). For the first anodic scan, an anodic peak current at 1.3 V (a_1) was observed, that corresponds to the oxidation of the adenine moiety in the NAD^+ molecule and formation of its oxidation products [2]. In the first cathodic scan, a cathodic peak was observed at potential of 0.07 V (c_1) that corresponded to the reduction of the NAD^+ oxidation products, which already produced at the first anodic scan. In the second scan, an anodic peak for correspondent cathodic peak was appeared at about 0.12 V (a_2, inset A, Fig. 1). As can be seen, the reversible redox system with $E^{0'}$ close to 0.1 V only observed when the first anodic scan was performed beyond the oxidation process (a_1). This oxidation product of NAD^+ (stated as Ox-P(NAD^+)) is strongly adsorbed on the electrode surface. The first and 250th recorded voltammograms obtained when the same electrode is subsequently removed from the cell, rinsed with water, and placed in a fresh buffer solution without NAD^+ (inset B in Fig. 1). As can be seen, the separation between cathodic and anodic peak potentials (ΔE_p) is about 40 mV and the ratio of cathodic peak current (i_{pc}) to anodic peak current (i_{pa}) exactly equals to unity. The redox system resulted from the adsorbed NAD^+ oxidation product is very stable and only 10% reduction in peak current happens after 250 repetitive cycles. Additionally, the storage stability of the chemically modified electrode was very good as the electrode was found to have reserved (95%) its initial activity for more than four weeks when kept in air at room temperature. This high stability may be ascribed to the chemical and mechanical stability of MWCNTs/IL nanocomposite as well as its compatibility with the NAD^+ oxidation product adsorbed on its surface which indicates the promising properties of MWCNTs/IL as a transducer for electrochemical oxidation of NAD^+ and entrapment of produced redox system.

Based on earlier investigations on purine oxidation [45–47] as well as their own findings, Alvarez-Gonzalez and coworkers proposed a mechanism for the electrochemical oxidation of NAD^+ [2]. The schematic of NAD^+ electrooxidation mechanism is presented here based on one described by Alvarez-Gonzalez (supplier information Scheme 1). The oxidation of the adenine moiety in NAD^+ proceeds by two sequential two-electron, two-proton oxidation steps to give the 2-hydroxyadeninedinucleotide (II) and the 2,8-dihydroxyadeninedinucleotide (III). Further removal by a two-electron, two-proton oxidation step results in the formation of the corresponding quinone-diimine (IV) stabilized by adsorption on

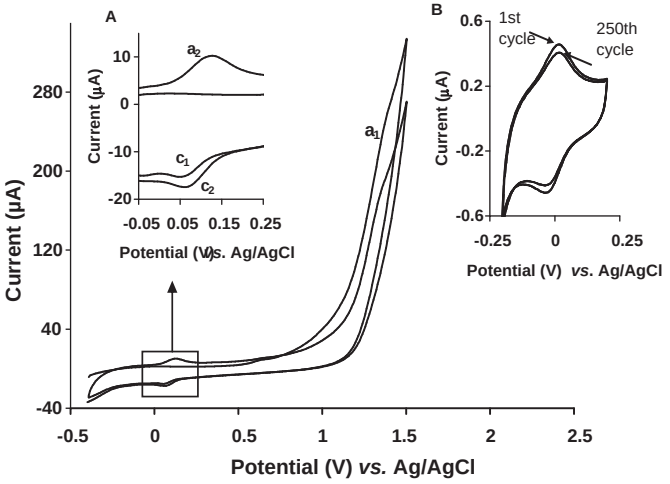

Fig. 1. The first and second recorded cyclic voltammograms of MWCNTs/IL modified GC electrode in 0.1 M PBS (pH 8.8) containing 1 mM NAD^+ at scan rate of 0.1 V s^{-1}. Inset (A): enlarged cyclic voltammograms of the defined region. Inset (B): the 1st and 250th recorded cyclic voltammograms of MWCNTs/IL/Ox-P(NAD^+) modified GC electrode in PBS (pH 8.8) at scan rate of 0.1 V s^{-1}.

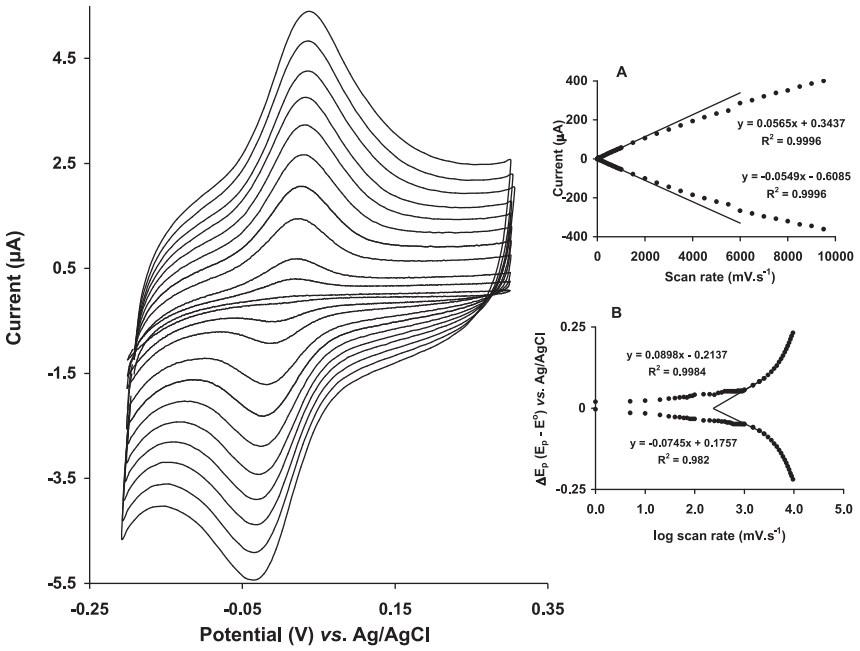

Fig. 2. Cyclic voltammetric responses of MWCNTs/IL/NAD$^+$ modified electrode in PBS solution, pH 8.8 at scan rates (inner to outer) 10, 20, 30, 40, 50, 60, 70, 80, 90, and 100 mV s^{-1}. Inset (A): plot of peak current vs. scan rate. Inset (B): variation of peak potential separation vs. log ν.

the electrode surface. Peak c_2 (Fig. 1 inset A) could therefore be due to the reversible reduction of the quinone-diimine back to 2,8-dihydroxyadeninedinucleotide. The electrocatalytic oxidation of NADH may be ascribed to this quinone-diimine species. As is well-known, this redox couple can act as electrocatalyst toward NADH oxidation.

Cyclic voltammograms of MWCNTs/IL/Ox-P(NAD$^+$) modified GC electrode at different scan rates were recorded (Fig. 2). The peak currents of the redox system are directly proportional to the scan rate for sweep rates below 1.5 V s^{-1} (inset A in Fig. 2) which confirms the adsorption nature of the electrochemical process. Moreover at higher sweep rates ($\nu > 1.5$ V s^{-1}), peak separations begin to increase (inset B in Fig. 2), indicating limitation due to the charge transfer kinetics. Based on the Laviron theory [48], the heterogeneous electron transfer rate constant (k_s) and charge transfer coefficient (α) can be determined by measuring the variation of peak potential with scan rate. The values of peak potentials were proportional to log(ν) for scan rates higher than 2.0 V s^{-1}. Using the equation $E_p = K - 2.303\ (RT/\alpha nF)\log \nu$, where $K = E^{0'} - 2.303(RT/\alpha nF)\log(RTk_s/nF)$, charge transfer coefficient (α) for proposed redox couple was calculated. Through introducing this value in the following Eq. (1), an apparent surface electron transfer rate constant (k_s) was estimated:

$$\log k_s = \alpha \log(1-\alpha) + (1-\alpha)\log\ \alpha - \log\left(\frac{RT}{nF\nu}\right) - \frac{\alpha(1-\alpha)nF\Delta E}{2.303RT} \quad (1)$$

The values of k_s and α were obtained as 9.8 ($\pm$0.30) s^{-1} and 0.36, respectively. The value of heterogeneous electron transfer rate constant indicates high ability of MWCNTs/IL nanocomposite for promoting electron transfer between redox couple and electrode surface. The large number of structural defects on the MWCNTs surface as well as its special nanostructure may act as molecular wires, enhance the direct electron transfer redox systems at MWCNTs/IL nanocomposite interface. The surface coverage concentration (Γ) of NAD$^+$ oxidation product was estimated by integrating the area under the anodic peak. According to the equation $\Gamma = Q/nFA$, the surface concentration of proposed molecule was about 1.15×10^{-10} ($\pm$0.20) mol cm^{-2}. These results indicate high loading ability of the MWCNTs/IL for immobilization of NAD$^+$ oxidation product. The electrochemical behavior of modified electrode in solutions with different pHs was also investigated (Fig. 3). As shown, well-defined and strongly pH dependent redox couple obtained for MWCNTs/IL/Ox-P(NAD$^+$) modified GC electrode in the pH range of 5–12. The formal potential was pH dependent, with a slope of 59 mV pH^{-1} ($E^{0'} = 0.5346 - 0.0586$ pH, $R^2 = 0.9975$, $n = 8$ where n is the number of different pHs used for obtaining the calibration equation), which well agrees with the anticipated Nernstian value for a two-electron and two-proton process.

3.2. Electrocatalytic oxidation of NADH on MWCNTs/IL/Ox-P(NAD$^+$) modified GC electrode

One of the main objectives of this study was to fabricate a modified electrode capable of the electrocatalytic oxidation of NADH. Due to the stability and electrochemical reversibility of generated redox couple at MWCNTs/IL/Ox-P(NAD$^+$) nanocomposite modified GC electrode, it can be used as a good mediator to shuttle electrons between electrode and NADH. In order to

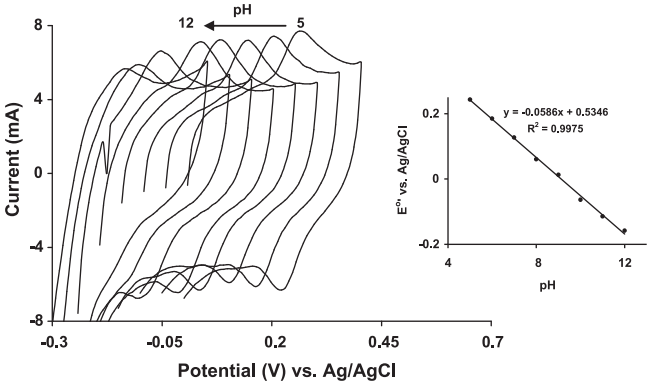

Fig. 3. Cyclic voltammograms of MWCNTs/IL/NAD$^+$ modified GC electrode at scan rate 0.1 V s^{-1} in PBS solutions with different pHs: from right to left 5–12. Inset: plot of formal potential vs. pH values.

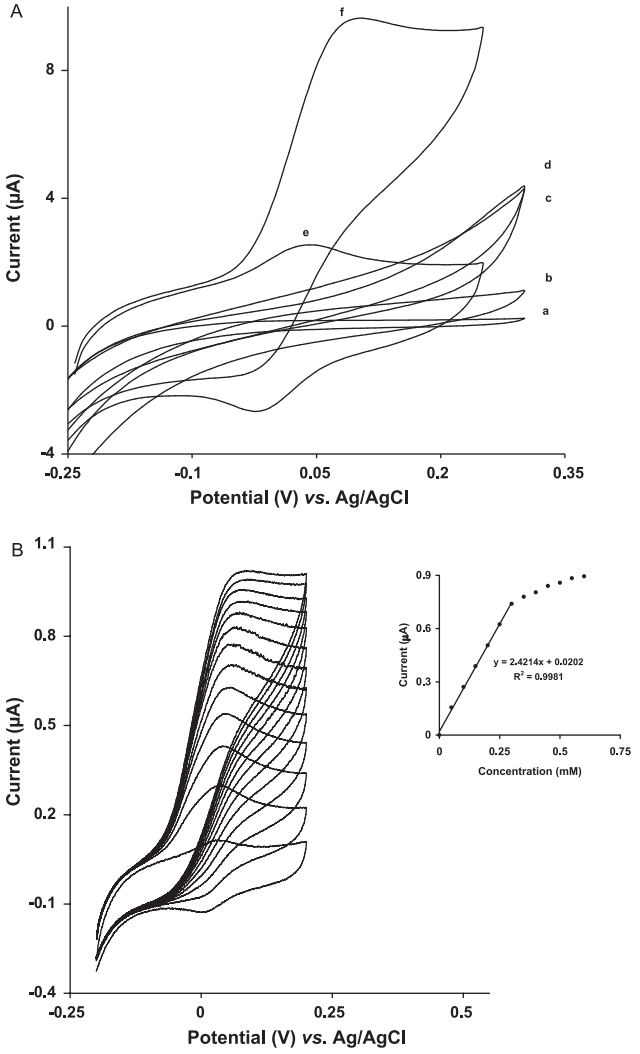

Fig. 4. (A) Cyclic voltammograms of MWCNTs (a and b), MWCNTs/IL (c and d) and MWCNTs/IL/Ox-P(NAD^+) (e and f) modified GC electrodes in PBS (pH 8.8) at scan rate of 50 mV s^{-1} in the absence (a, c and e) and presence (b, d and f) of 1×10^{-3} mol L^{-1} NADH. (B): Cyclic voltammograms of MWCNTs/IL/Ox-P(NAD^+) modified GC electrode in PBS (pH 8.8) solution at different concentrations of NADH and scan rate 0.01 V s^{-1} (from inner to outer) 0, 5, 10, 15, 20, 25, 30, 35, 40, 45, 50, 55, 60 ($\times 10^{-5}$ mol L^{-1}). Inset is the plot of catalytic current vs. NADH concentrations.

examine the electrocatalytic activity of the modified electrode, the cyclic voltammograms were obtained in the absence and presence of 1×10^{-3} mol L^{-1} NADH at MWCNTs, MWCNTs/IL and MWCNTs/IL/Ox-P(NAD^+) modified GC electrodes in PBS (pH 8.8) at 0.1 V s^{-1}. As shown in Fig. 4A (voltammograms a–d) for MWCNTs and MWCNTs/IL modified GC electrodes, no response was observed in the absence and presence of NADH in the potential range from −0.2 to 0.3 V, while for MWCNTs/IL/Ox-P(NAD^+) modified GC electrode, a marked enhancement in the anodic current as well as reduction in cathodic current was observed upon addition of NADH (voltammogram f) which indicates a strong electrocatalytic activity of the modified electrode toward NADH oxidation. Furthermore, cyclic voltammograms of MWCNTs/IL/Ox-P(NAD^+) modified GC electrode in PBS containing different concentrations of NADH were recorded (Fig. 4B). As shown in this figure, there is a notable enhancement of anodic peak currents at potentials close to the formal potential of redox couple ($E^{0'} = 0.05$ V) along with a decrease in the cathodic current with successive additions of NADH. The variation of catalytic peak currents vs. NADH concentration was recorded (inset in Fig. 4B). The catalytic currents linearly

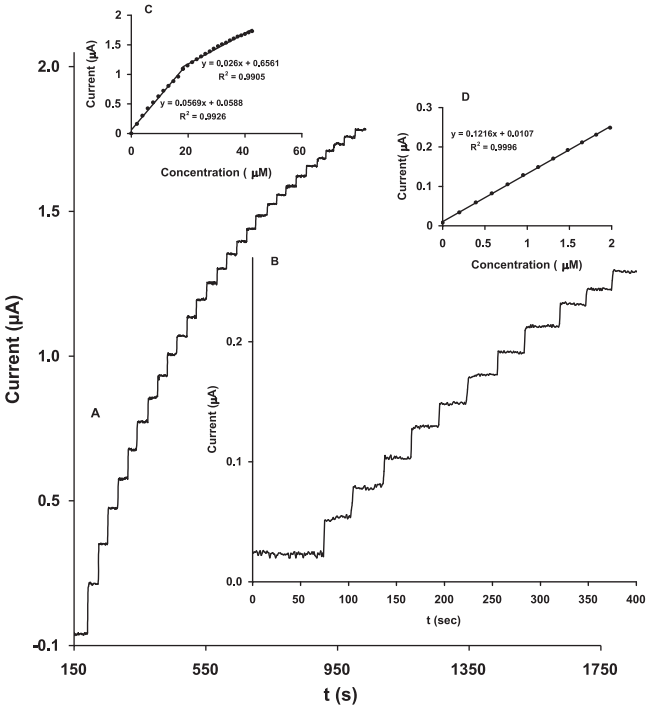

Fig. 5. (A) Amperometric response of rotating MWCNTs/IL/Ox-P(NAD^+) modified GC electrode to successive additions of 2×10^{-6} mol L^{-1} NADH, at applied potential of 0.1 V, PBS (pH 8.8) and rotation speed is 400 rpm. (B) Successive additions of 2×10^{-7} mol L^{-1} NADH. (C and D) plots of chronoamperometric current vs. NADH concentration.

increased with increasing the NADH concentration in the range of 5×10^{-5}–3×10^{-4} mol L^{-1} which can be fitted into the equation; I_p (μA) = 2.4214[NADH]($\times 10^{-3}$ mol L^{-1}) + 0.0202 μA and $R^2 = 0.9981$.

Fig. 5 presents the amperometric response of the MWCNTs/IL/Ox-P(NAD^+) modified GC electrode at +0.1 V to the successive additions of NADH in 0.1 mol L^{-1} PBS (pH 8.8). Immediately after the addition of NADH, the anodic current increased and reached a steady state within 5 s. The response displayed two linear concentration ranges; one from 2×10^{-7} to 2×10^{-5} mol L^{-1} with a correlation coefficient of 0.9926 and sensitivity of 0.44 (±0.02) A mol^{-1} L cm^{-2} and another from 2×10^{-5} to 4.2×10^{-5} mol L^{-1} with a correlation coefficient of 0.9905 and sensitivity of 0.2 (±0.01) A mol^{-1} L cm^{-2}. The calculated detection limit is 2×10^{-8} mol L^{-1} based on signal to noise ratio of 3. The obtained detection limit is significantly lower compared to most previously reported values of 1×10^{-7} mol L^{-1} for nafion/CNTs/DHB/GC [49], 1.5×10^{-7} mol L^{-1} for meldola's blue adsorbed on $SiO_2/SnO_2/Sb_2O_5$ [50], 1×10^{-6} mol L^{-1} for thionine adsorbed on nafion/CNTs/GC [51], 5×10^{-8} mol L^{-1} for boron doped CNTs/GC [52] and 6×10^{-8} mol L^{-1} for MWCNTs/IL/chitosan/GC [43].

Another attractive feature of our proposed electrode was its highly stable amperometric response to NADH. The amperometric responses of an unmodified and a MWCNTs/IL/Ox-P(NAD^+) modified GC electrode to 2×10^{-5} mol L^{-1} NADH recorded over a continuous period of 1800 s (supplier information S.2). At the unmodified electrode, the applied potential was held at +0.75 V for NADH oxidation. The bare GC electrode displayed a rapid decay of the signal with up to 70% current depressions after 1800 s, indicating a nearly complete inhibition of the oxidation process. In contrast, the response of the MWCNTs/IL/NAD^+ modified GC electrode remained nearly stable with only 15% current diminutions at 1800 s. Obviously the oxidation of NADH at the bare GC led to surface passivation resulted from the radical intermediates [9],

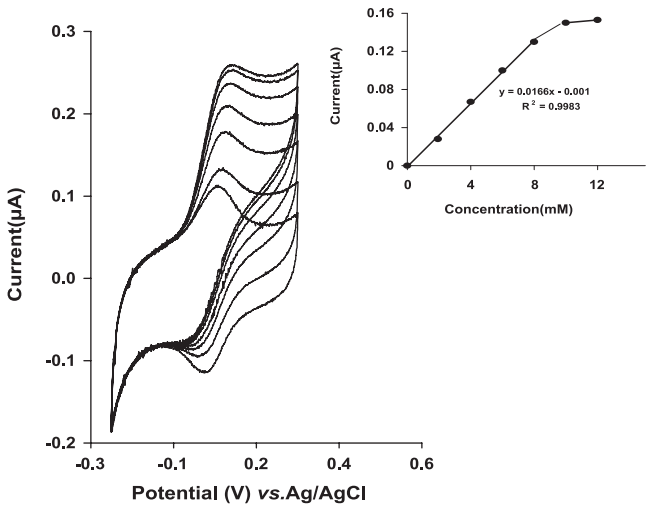

Fig. 6. Cyclic voltammograms of MWCNTs/IL/Ox-P(NAD^+) modified GC electrode in PBS (pH 8.8) containing 1×10^{-3} mol L^{-1} of each NAD^+ and ADH compounds at different concentrations of ethanol and scan rate of 10 mV s^{-1} (from inner to outer) 0, 2, 4, 6, 8, 10 and 12 ($\times 10^{-3}$ mol L^{-1}). Inset is the plot of catalytic current vs. ethanol concentrations.

the oxidation products formed at a high overpotential. The surface fouling caused the loss of analytical sensitivity and reproducibility. However, the MWCNTs/IL/Ox-P(NAD^+) modified GC electrode overcame this drawback due to the improved kinetics of electron transfer and more negative potential applied for the oxidation of NADH (0.1 V), which greatly limited the amount of radical intermediates and their dimerization. The operational stability of MWCNTs/IL/Ox-P(NAD^+) modified GC electrode was also examined by performing successive amperometric measurements at 0.1 mol L^{-1} PBS (pH 8.8) upon injection of 1×10^{-5} mol L^{-1} NADH. After 100 successive measurements, no change was detected in the response of the modified electrode. The MWCNTs/IL/Ox-P(NAD^+) modified GC electrode also possess a good storage stability. The electrode response for 1×10^{-5} mol L^{-1} NADH was measured every day, then it was stored at room temperature. The results indicated, only 10% reduction in response was observed after more than 15 days (supplier information S.3). Thus, the nanocomposite was an excellent electrocatalytic material for sensitive and stable amperometric detection of NADH.

3.3. Ethanol biosensing on MWCNTs/IL/NAD^+ modified GC electrode

In order to further confirm the usefulness of the described electrocatalytic system, its ability as an ethanol biosensor was examined. In general, dehydrogenase-based enzymes require NAD^+ as a cofactor for enzymatic reaction so that NAD^+ could be reduced to NADH simultaneously with oxidation of analyte [2]. The ethanol biosensor is based on the reaction sequence outlined in Scheme 1. Fig. 6 shows the cyclic voltammograms of MWCNTs/IL/Ox-P(NAD^+) modified GC electrode in 0.1 mol L^{-1} PBS (pH 8.8) containing 1×10^{-3} mol L^{-1} of each NAD^+ and ADH as well as different concentrations of ethanol. As indicated, the anodic peak current increased and cathodic peak disappeared with increasing ethanol concentration. The catalytic currents linearly increased with increasing ethanol concentration in the range up to 1×10^{-2} mol L^{-1} with sensitivity of 128 (± 6) μA mol^{-1} L cm^{-2}.

Additionally, amperometric responses of MWCNTs/IL/Ox-P(NAD^+) modified GC electrode to different concentrations of ethanol were recorded (Fig. 7A). This observation clearly supports the fact that the increase of current response upon successive additions of ethanol is due to the oxidation of enzymatically produced

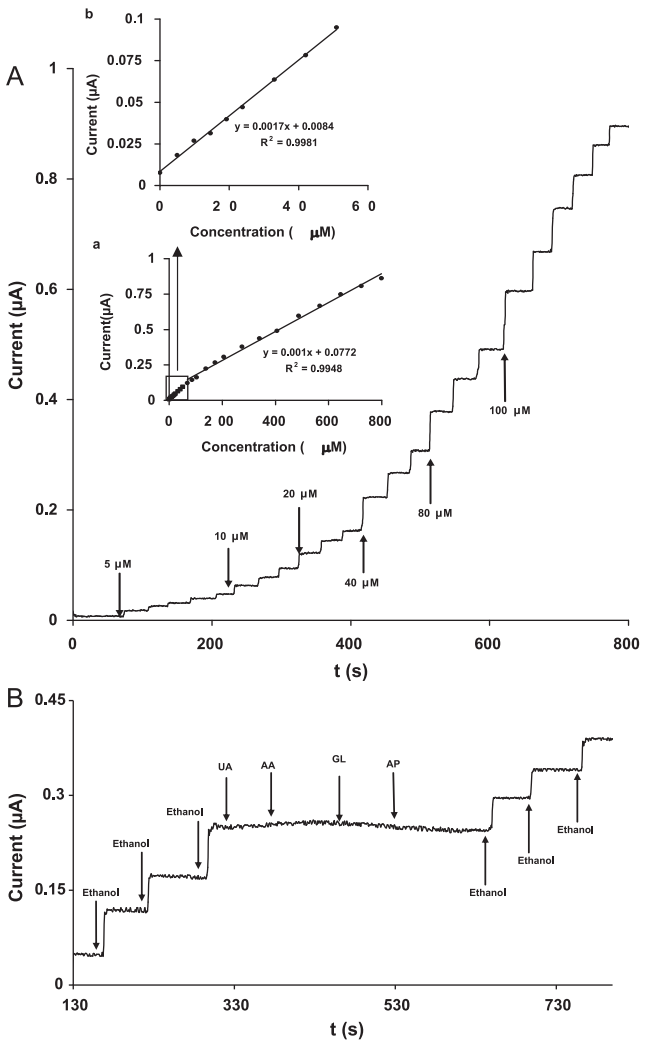

Fig. 7. (A) Chronoamperometric response of MWCNTs/IL/Ox-P(NAD^+) modified GC electrode in 1×10^{-3} mol L^{-1} NAD^+ and 1×10^{-3} mol L^{-1} ADH, 0.1 mol L^{-1} PBS (pH 8.8) on injecting different concentrations of ethanol at working potential of 0.1 V vs. Ag/AgCl. Inset (a): plot of amperometric response vs. ethanol concentrations and inset (b) is the enlarged view of the defined segment in inset a. (B) Amperometric response of the MWCNTs/IL/Ox-P(NAD^+) modified GC electrode in 0.1 mol L^{-1} PBS (pH 8.8) containing 5×10^{-5} mol L^{-1} ethanol, 1×10^{-3} mol L^{-1} NAD^+ and 1×10^{-3} mol L^{-1} ADH spiked with UA (0.1 mM), AA (0.1 mM), AP (0.1 mM), and GL (0.1 mM).

NADH during ethanol oxidation. The response of the biosensor was fast, and the response time was ca. 10 s. Under optimal conditions, the biosensor response increased with increasing ethanol concentration in two concentration ranges. In the EtOH concentration range of 5×10^{-6}–6×10^{-5} mol L^{-1}, the regression equation was I (nA) = 1.7 [EtOH]($\times 10^{-6}$ mol L^{-1}) + 8.3 nA and the correlation coefficient was 0.9981. The detection limit was calculated as 5×10^{-7} mol L^{-1} based on signal to noise ratio of 3. For higher concentration range of ethanol, 6×10^{-5}–9×10^{-4} mol L^{-1}, the regression equation was I (nA) = 1.0 [EtOH]($\times 10^{-6}$ mol L^{-1}) + 77.2 nA with correlation coefficient of 0.9948.

The effect of pH of contact solution on the current responses of MWCNTs/IL/Ox-P(NAD^+) modified GC electrode was studied over the pH range of 7.0–9.0 in order to see how it affects the activity of the sensing layer. The amperometric currents obtained at different pH values for 2×10^{-5} mol L^{-1} ethanol in 0.1 mol L^{-1} PBS containing 1×10^{-3} mol L^{-1} of each NAD^+ and ADH showed that the amperometric response at pH 8.8 was somewhat higher than other pHs and therefore PBS at pH 8.8 was used throughout experiments (supplier

Table 1
Response characteristics of different dehydrogenase-based ethanol biosensors.[a]

Biosensors	Response time (s)	Dynamic range ($\times10^{-3}$ mol L^{-1})	Sensitivity (mA mol^{-1} L cm^{-2})	Applied potential (V)
IL/graphene/chitosan/GC [3]	20	0.025–0.2	6.91	0.45 (Ag/AgCl)
MWCNTs/MB/GC [12]	n.d.[b]	0.05–10	4.75	0.00 (SCE)
MB/OMC/GC [55]	7 ± 1	Up to 6	0.035	−0.10 (Ag/AgCl)
CNF/GC [56]	10	0.01–0.425	n.d.	0.06 (SCE)
Nafion/PDDA/SWNTs/GC [57]	5	0.5–5	n.d.	0.10 (SCE)
MWCNTs/titania/Nafion/GC [58]	2	0.01–50	51.6	0.50 (Ag/AgCl)
PVA/MWCNTs/GC [59]	8	Up to 1.5	0.196	0.70 (Ag/AgCl)
PEDOT/PSS/Au_{nano}/ITO [24]	5	0.001–0.1	97	0.04 (SCE)
SNMB/NAD^+/GC [60]	n.d.	0.1–10	2.33	0.00 (SCE)
PBCB/SWNT/GC [61]	n.d.	0.4–2.4	n.d.	0.00 (SCE)
MWCNTs/IL/CPZ [44]	–[c]	0.04–1.5	1.97	0.30 (Ag/AgCl)
1,2-Diaminobenzene-nanotubes/GC [62]	n.d.	0.05–1.0	0.099	0.45(Ag/AgCl)
MWCNTs/IL/NAD^+/GC [this study]	10	0.005–0.06	13.1	0.10 (Ag/AgCl)
		0.06–0.9	7.7	0.10 (Ag/AgCl)

[a] IL, ionic liquid; MWCNTs; multiwalled carbon nanotubes; MB, meldola's blue; OMC, ordered mesoporous carbon; CNF, carbon nanofiber; PDDA, poly(dimethyldiallylammonium chloride); SWNTs, single walled carbon nanotubes; PVA, poly vinyl alcohol; PEDOT, poly (3,4-ethylenedioxythiophene); PSS, poly (styrene sulfonic acid); Au_{nano}, gold nanoparticles; ITO, indium-doped tin oxide; SNMB, meldola's blue adsorbed on silica gel modified with niobium oxide; PBCB, poly (brilliant cresyl blue); CPZ, chloropromazine oxidation product.
[b] n.d., data not determined.
[c] Differential pulse voltammetric method was used.

information S.4). This result is comparable with the other reported results of 8.6 for the multiwalled carbon nanotube/chitosan/ADH nanobiocomposite [53] or 8.5 for the o-phenylenediamine modified carbon paste [54] ethanol biosensors. Table 1 lists the response characteristics such as response time, dynamic range, sensitivity and applied potential of the proposed ethanol biosensor in this work compared to the some other ethanol biosensors reported in the literature. The results presented in Table 1 obviously show that the different characteristics of the proposed ethanol biosensor based on MWCNTs/IL/Ox-P(NAD^+) nanocomposite modified GC electrode are better in some cases or comparable with the other biosensors that have been reported so far.

3.4. Investigation of interfering substances and real sample analysis

The common problem in the electrochemical determination of ethanol is the interference from redox active species, such as ascorbic acid (AA), uric acid (UA), glucose (GL) and acetaminophen (AP). The effects of these common interfering species on the amperometric response of electrode were evaluated (Fig. 7B). The addition of 1×10^{-4} mol L^{-1} of each of AA, UA, GL and AP compounds almost did not cause any interference on the current response. In fact, even the 100 fold concentrations of UA, GL and AP with respect to ethanol were added and the observed response was negligible. However, when concentrations higher than 1×10^{-4} mol L^{-1} of AA were added, its response would be comparable with the ethanol response. Nevertheless, the concentration of AA in real samples rarely is so high that leads to significant interference. The use of a low operating potential greatly reduced the interference; and thus, highly selective response to ethanol was obtained without the use of perm-selective membrane. This obviously is another advantage of the proposed biosensor.

Table 2
Determination of ethanol in real samples using MWNTs/IL/NAD^+ modified GC electrode.

Sample No.	Spiked ($\times10^{-6}$ mol L^{-1})	Found ($\times10^{-6}$ mol L^{-1})	Recovery (%)
1 (apple Istak)	0.00	0.00	97.60 (±2.40)
	100.00	97.60 ± 2.40[a]	
2 (lemon Istak)	0.00	0.00	97.20 ± 2.50
	100.00	97.20 ± 2.50	
3 (lemon Delster)	0.00	0.00	98.1 ± 2.90
	100.00	98.1 ± 2.90	

[a] The mean value for three measurements.

In order to estimate the applicability of the methodology, the proposed ethanol biosensor was tested by applying it to the measurement of ethanol concentration in real samples. The obtained results were given in Table 2. It could be seen that there is a good agreement between the spiked and found values for detection of ethanol. These results clearly indicate that the system presented in this work to be valid for the analysis of ethanol in real samples.

4. Conclusion

The electrochemical oxidation of NAD^+ at MWCNTs/IL modified GC electrode gives rise to redox active products which strongly adsorbed at nanocomposite surface. Due to unique properties of MWCNTs/IL nanocomposite and generated redox couple as well as synergistic effects exist between different components of the proposed system, the electrochemical properties of produced nanocomposite significantly improved and the modified electrode shows a stable and reproducible redox system with long operational and storage stability and excellent electrochemical reversibility. Under operational conditions, one of the products resulted from the oxidation of adenine moiety in NAD^+ molecule shows excellent electrocatalytic activity toward NADH oxidation with significantly lowering the overpotential compared to bare GC electrode. This electrocatalytic response of MWCNTs/IL/Ox-P(NAD^+) modified GC electrode exhibits a linear dependency on the NADH concentration, with a limit of detection of 2×10^{-8} mol L^{-1} and wide linear range of 2×10^{-7}–4.2×10^{-5} mol L^{-1}. The analytical performance as well as the stability of its NADH response demonstrated that MWCNTs/IL/Ox-P(NAD^+) modified GC electrode would be suitable for the assembly of amperometric NADH sensors. In order to examine the mentioned electrocatalytic system, its ability to ethanol sensing was investigated by cyclic voltammetry and chronoamperometric methods. The obtained results further demonstrated its good analytical performance with low cost, convenient preparation along with sensitive and rapid detection. The high sensitivity, linear range, reproducibility, and the minimal surface fouling combined with the attractive low potential of the NADH oxidation make this nanobiocomposite electrode an extremely promising candidate to serve as the electrochemical substrate for fabrication of biosensors that incorporate dehydrogenase enzymes.

Thus, such MWCNTs/IL/Ox-P(NAD^+) nanocomposite is an attractive amperometric transducer in fabrication of electrochemical sensors and biosensors.

Acknowledgements

This research was supported by the Iranian Nanotechnology Initiative and the Research Offices of the University of Kurdistan and University of Tarbiat Modarres.

Appendix A. Supplementary data

Supplementary data associated with this article can be found, in the online version, at doi:10.1016/j.talanta.2012.01.003.

References

[1] Q. Wu, M. Maskus, F. Pariente, F. Tobalina, V.M. Fernandez, E. Lorenzo, H.D. Abruna, Anal. Chem. 68 (1996) 3688–3696.
[2] M.I. Alvarez-Gonzalez, S.B. Saidman, M.J.L. Castanon, A.J.M. Ordieres, P.T. Blanco, Anal. Chem. 72 (2000) 520–527.
[3] C. Shan, H. Yang, D. Han, Q. Zhang, A. Ivaska, L. Niu, Biosens. Bioelectron. 25 (2010) 1504–1508.
[4] L. Meng, P. Wu, G. Chen, C. Cai, Y. Sun, Z. Yuan, Biosens. Bioelectron. 24 (2009) 1751–1756.
[5] M.M. Rahman, M.J.A. Shiddiky, M.D.A. Rahman, Y.D. Shim, Anal. Biochem. 384 (2009) 159–165.
[6] W.M. Clark, Oxidation-Reduction Potentials of Organic Systems, William and Wilkins, Baltimore, MD, 1960.
[7] J. Moiroux, P.J. Elving, Anal. Chem. 50 (1978) 1056–1062.
[8] A. Ciszewski, G. Milczarek, Anal. Chem. 72 (2000) 3203–3209.
[9] A.A. Karyakin, E.E. Karyakin, W. Schuhmann, H.L. Schmidt, Electroanalysis 11 (1999) 553–557.
[10] N. de los Santos Alvarez, M.J. Lobo Castanon, A.J. Miranda Ordieres, P. Tunon Blanco, H.D. Abruna, Anal. Chem. 77 (2005) 2624–2631.
[11] C.M. Maroneze, L.T. Arenas, R.C.S. Luz, E.V. Benvenutti, R. Landers, Y. Gushikem, Electrochim. Acta 53 (2008) 4167–4175.
[12] A.S. Santos, A.C. Pereira, N. Duran, L.T. Kubota, Electrochim. Acta 52 (2006) 215–220.
[13] L. Zhu, R.J. Yang, X. Jiang, D. Yang, Electrochem. Commun. 11 (2009) 530–533.
[14] R.C.S. Luz, F.S. Damos, A.A. Tanaka, Y. Kubota, L.T. Gushikem, Electrochim. Acta 53 (2008) 4706–4714.
[15] M.A. Ghanem, J.M. Chretien, J.D. Kilburn, P.N. Bartlett, Bioelectrochemistry 76 (2009) 115–125.
[16] A. Salimi, R. Hallaj, M. Ghadermazi, Talanta 65 (2005) 888–894.
[17] D. Gligor, F. Balaj, A. Maicaneanu, R. Gropeanu, I. Grosu, L. Muresan, I.C. Popescu, Mater. Chem. Phys. 113 (2009) 283–289.
[18] A.S. Santos, M. Ortea, A.M. Paneda, M.J.L. Castanon, A.J.M. Ordieres, Blanco, J. Electroanal. Chem. 502 (2001) 109–117.
[19] A. Balamurugan, S.M. Chen, Sens. Actuators B 129 (2008) 850–858.
[20] N. de los Santos Alvarez, P. Muniz Ortea, A. Montes Paneda, M.J. Lobo Castanon, A.J. Miranda Ordieres, P. Tunon Blanco, J. Electroanal. Chem. 502 (2001) 109–117.
[21] D. Gligor, Y. Dilgin, I.C. Popescu, L. Gorton, Electrochim. Acta 54 (2009) 3124–3128.
[22] S. Mu, Y. Zhang, J. Zhai, Electrochem. Commun. 11 (2009) 1960–1963.
[23] A.A. Karyakin, Y.N. Ivanova, E.E. Karyakina, Electrochem. Commun. 5 (2003) 677–680.
[24] K.M. Manesh, P. Santhosh, A. Gopalan, K.P. Lee, Talanta 75 (2008) 1307–1314.
[25] K.C. Lin, S.M. Chen, J. Electroanal. Chem. 589 (2006) 52–59.
[26] J.J. Gooding, R. Wibowo, J.Q. Liu, W.R. Yang, D. Losic, S. Orbong, F.J. Mearns, J. Am. Chem. Soc. 125 (2003) 9006–9007.
[27] C.N.R. Rao, B.C. Satishkumar, A. Govindaraj, M. Nath, Chem. Phys. Chem. 2 (2001) 78–105.
[28] R.H. Baughman, A.A. Zakhidov, W.A. de Heer, Science 297 (2002) 787–792.
[29] Q. Zhao, Z. Gan, Q. Zhuang, Electroanalysis 14 (2002) 1609–1613.
[30] M. Musameh, J. Wang, A. Merkoci, Y.H. Lin, Electrochem. Commun. 4 (2002) 743–746.
[31] M.G. Zhang, W. Gorski, Anal. Chem. 77 (2005) 3960–3965.
[32] R.J. Chen, Y. Zhang, D. Wang, H. Dai, J. Am. Chem. Soc. 123 (2001) 3838–3839.
[33] A. Salimi, A. Noorbakhsh, S. Soltanian, Electroanalysis 18 (2006) 703–711.
[34] A. Salimi, H. Mamkhezri, S. Mohebbi, Electrochem. Commun. 8 (2006) 688–696.
[35] A. Salimi, H. Mamkhezri, R. Hallaj, S. Zandi, Electrochim. Acta 52 (2007) 6097–6105.
[36] A. Salimi, L. Miranzadeh, R. Hallaj, Talanta 75 (2008) 147–156.
[37] D. Li, M.B. Muller, S. Gilje, R.B. Kaner, G.G. Wallace, Nat. Nanotechnol. 3 (2008) 101–105.
[38] Y. Zhang, Y. Shen, J. Yuan, D. Han, Z. Wang, Q. Zhang, K. Niu, Angew. Chem. Int. Ed. 45 (2006) 5867–5870.
[39] M.C. Buzzeo, R. Evans, R.G. Compton, Chem. Phys. Chem. 5 (2004) 1106–1120.
[40] D. Wei, A. Ivaska, Anal. Chim. Acta 607 (2008) 126–135.
[41] H. Liu, P. He, C. Sun, L. Shi, Y. Liu, G. Zhu, J. Li, Electrochem. Commun. 7 (2005) 1357–1363.
[42] T. Fukushima, A. Kosaka, Y. Ishimura, T. Yamamoto, T. Takigawa, N. Ishii, T. Aida, Science 300 (2003) 2072–2074.
[43] Q. Wang, H. Tang, Q. Xie, L. Tan, Y. Zhang, B. Li, S. Yao, Electrochim. Acta 52 (2007) 6630–6637.
[44] A. Salimi, S. Lashgari, A. Noorbakhsh, Electroanalysis 22 (2010) 1707–1716.
[45] G. Dryhurst, P.J. Elving, J. Electrochem. Soc. 115 (1968) 1014–1020.
[46] G. Dryhurst, Electrochemistry of Biological Molecules, Academic Press, New York, 1977.
[47] R.N. Goyal, A. Kumar, A. Mittal, J. Chem. Soc., Perkin Trans. 2 (1991) 1369–1375.
[48] E. Laviron, J. Electroanal. Chem. 101 (1979) 19–28.
[49] C.R. Raj, S. Chakraborty, Biosens. Bioelectron. 22 (2006) 700–706.
[50] T.C. Canevary, R.C.G. Vinhas, R. Landers, Y. Gushikem, Biosens. Bioelectron. 26 (2011) 2402–2406.
[51] M. Huang, H. Jiang, J. Zhai, B. Liu, S. Dong, Talanta 74 (2007) 132–139.
[52] C. Deng, J. Chen, X. Chen, C. Xiao, Z. Nie, S. Yao, Electrochem. Commun. 10 (2008) 907–909.
[53] C.A. Lee, Y.C. Tsai, Sens. Actuators B 138 (2009) 518–523.
[54] M.J. Lobo, A.J. Miranda, P. Tunon, Biosens. Bioelectron. 12 (1997) 511–520.
[55] X. Jiang, L. Zhu, D. Yang, X. Mao, Y. Wu, Electroanalysis 21 (2009) 1617–1623.
[56] L. Wu, X. Zhang, H. Ju, Anal. Chem. 79 (2007) 453–458.
[57] S. Liu, C. Cai, J. Electroanal. Chem. 602 (2007) 103–114.
[58] H.N. Choi, Y.K. Lyu, J.H. Han, W.Y. Lee, Electroanalysis 19 (2007) 1524–1530.
[59] Y.C. Tsai, J.D. Huang, C.C. Chiu, Biosens. Bioelectron. 22 (2007) 3051–3056.
[60] A.S. Santos, R.S. Freire, L.T. Kubota, J. Electroanal. Chem. 547 (2003) 135–142.
[61] D.W. Yang, H.H. Liu, Biosens. Bioelectron. 25 (2009) 733–738.
[62] F. Valentini, A. Salis, A. Curulli, G. Palleschi, Anal. Chem. 76 (2004) 3244–3248.